iScience

CellPress
OPEN ACCESS

Article

Efficacy of a cysteine protease inhibitor compared with enalapril in murine heart failure models

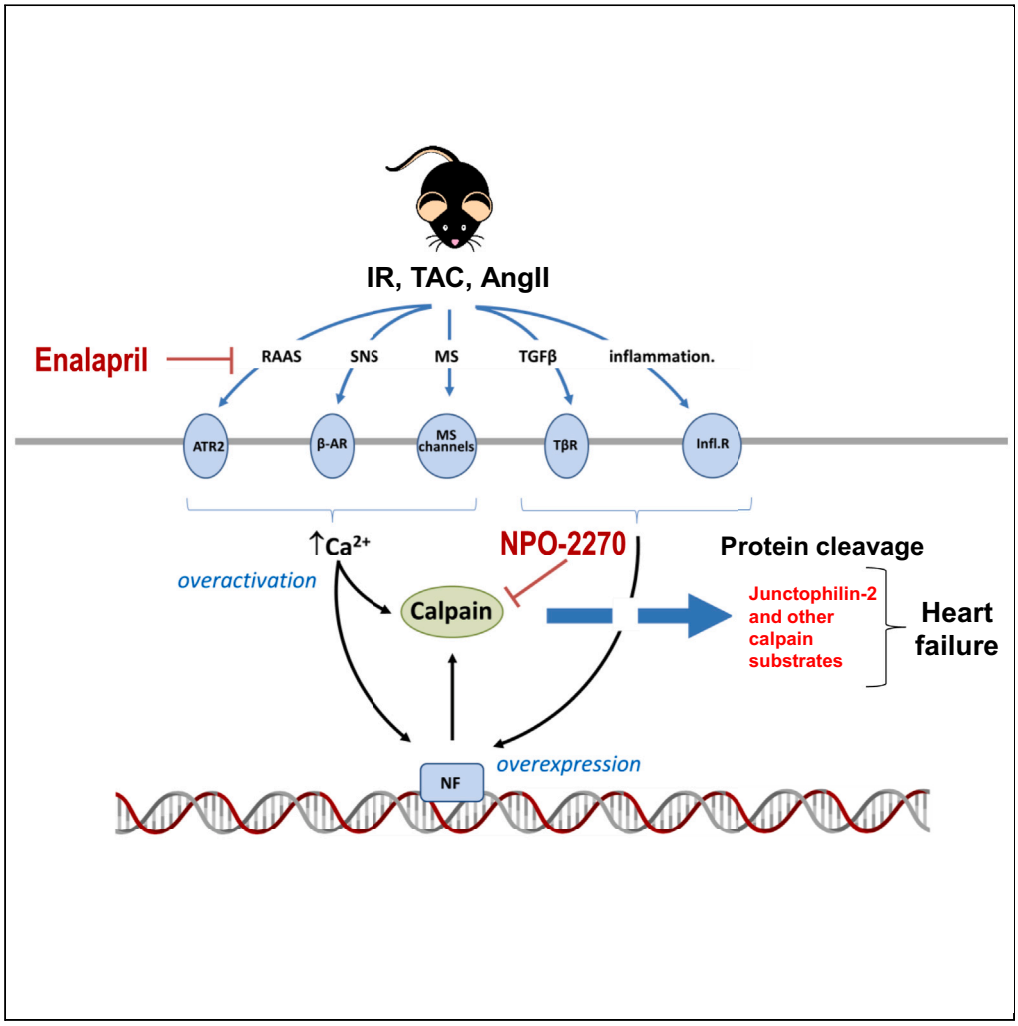

David Aluja, Sara Delgado-Tomás, Jose A. Barrabés, ..., Long-Sheng Song, Ignacio Ferreira-González, Javier Inserte

iferreir@vhebron.net (I.F.-G.)
javier.inserte@vhir.org (J.I.)

Highlights

NPO-2270 is a potent and selective cysteine protease inhibitor

NPO-2270 limits myocardial infarction and prevents adverse remodeling progression

NPO-2270 ameliorates cardiac dysfunction more effectively than enalapril

Effects of NPO-2270 correlate with reduced calpain cleavage of junctophilin-2

Aluja et al., iScience 27, 110935
October 18, 2024
https://doi.org/10.1016/j.isci.2024.110935

iScience

CellPress
OPEN ACCESS

Article

Efficacy of a cysteine protease inhibitor compared with enalapril in murine heart failure models

David Aluja,[1,2,3] Sara Delgado-Tomás,[1,2] Jose A. Barrabés,[1,2,3] Elisabet Miró-Casas,[1,2,3] Marisol Ruiz-Meana,[1,2,3] Antonio Rodríguez-Sinovas,[1,2,3] Begoña Benito,[1,2,3] Jinxi Wang,[4] Long-Sheng Song,[4] Ignacio Ferreira-González,[1,2,5,*] and Javier Inserte[1,2,3,6,*]

SUMMARY

Cysteine proteases calpains contribute to heart failure (HF), but it remains unknown whether their inhibition provides any benefit compared to standard pharmacological treatment for HF. Here, we characterize the pharmacological properties of NPO-2270 (NPO) as a potent inhibitor of cysteine proteases. Then, we describe that acute administration of NPO in rodent models of transient ischemia at the time of reperfusion reduces myocardial infarction, while its chronic oral administration attenuates adverse remodeling and cardiac dysfunction induced by ischemic and non-ischemic pathological stimuli more effectively than enalapril when given at the same dose. Finally, we provide evidence showing that the effects of NPO correlate with calpain inhibition and the preservation of the T-tubule morphology, due at least in part to reduced cleavage of the calpain substrate junctophilin-2. Together, our data highlight the potential of cysteine protease inhibition with NPO as a therapeutic strategy for the treatment of heart failure.

INTRODUCTION

Heart failure (HF) is a major health and economic challenge worldwide. Despite current pharmacological treatments in patients with HF delay disease progression and death, HF is still burdened by high morbidity and mortality.[1] Thus, new strategies to understand the complex mechanisms of HF and the identification of new targets are needed.

Calpains are a family of non-lysosomal cysteine proteases with essential functions in physiological Ca^{2+}-dependent processes.[2] Among them, calpain-1 and calpain-2 isoforms are ubiquitously expressed and tightly regulated mainly by their endogenous inhibitor calpastatin and the intracellular Ca^{2+} concentration. Numerous studies demonstrate that in those pathological conditions associated with Ca^{2+} overload, as occurs during the acute phase of myocardial ischemia/reperfusion, calpains are dysregulated and contribute to cardiomyocyte cell death through the proteolysis of a wide variety of proteins.[3,4] In addition, calpain-1 and calpain-2 are overexpressed and overactivated in hearts of patients with HF of different etiologies[5,6] and in multiple experimental models of HF.[6–9] The use of genetic mouse models with cardiac loss-of-function or gain-of-function, suggest their causal contribution to the inflammatory, hypertrophic, and fibrotic processes that characterize myocardial remodeling and cardiac dysfunction.[10–14] Various mechanisms related to the proteolysis of different calpain substrates have been proposed to explain their contribution to these effects.[15,16]

However, although targeting calpain activity appears promising, only few pre-clinical studies have explored the use of pharmacological calpain inhibitors as a therapeutic strategy to antagonize cardiac remodeling and its progression to HF, mainly due to the pharmacological limitations of available inhibitors.[6,8] More importantly, none of these studies have validated the potential of calpain inhibitors to enter in clinical trials by comparing their efficacy with conventional pharmacological HF treatments.

In the present study, we first identified NPO-2270 (NPO), a dipeptidyl ketoamide derivative synthesized and described by Landsteiner Genmed,[17] as a potent inhibitor of cysteine proteases with good oral bioavailability. Then, we determined its therapeutic potential in murine models of acute myocardial infarction and of adverse myocardial remodeling and HF and compared its efficacy with the ACE inhibitor enalapril. ACE inhibitors are still recommended by clinical practice guidelines as first-line therapy for the treatment of HF[18] and enalapril has been the drug of choice as a comparator in studies that analyzed the potential of new drugs in this clinical context.[19–21] Finally, we examined the effect of NPO and enalapril in preserving the T-tubule structure.

[1]Cardiovascular Diseases Research Group, Vall d'Hebron University Hospital and Research Institute, 08035 Barcelona, Spain
[2]Universitat Autònoma de Barcelona, 08193 Bellaterra, Spain
[3]CIBER de Enfermedades Cardiovasculares (CIBERCV), 28029 Madrid, Spain
[4]Division of Cardiovascular Medicine, Department of Internal Medicine, Carver College of Medicine, University of Iowa, Iowa City, IA 52242, USA
[5]CIBER de Epidemiología y Salud Pública (CIBERESP), 28029 Madrid, Spain
[6]Lead contact
*Correspondence: iferreir@vhebron.net (I.F.-G.), javier.inserte@vhir.org (J.I.)
https://doi.org/10.1016/j.isci.2024.110935

Table 1. NPO-2270 IC_{50} values (nmol/L)

Protease	IC_{50}
Calpain-1	51
Calpain-2	41
Cathepsin B	81
Cathepsin K	19
Cathepsin L	44
Cathepsin S	5
Cathepsin V	12

RESULTS

Pharmacological profile and preliminary safety and toxicology analyses of NPO-2270

The analysis of the *in vitro* protease inhibitory activity evaluated using standard fluorescence assays shows that NPO is a potent inhibitor of calpain-1 and calpain-2 and related cathepsins S, V, K, L, and B, with a calculated IC_{50} in the nanomolar range (Table 1).

Pharmacokinetic data are shown in Table 2. Following a single intravenous administration of 1 mg/kg NPO to C57BL/6J mice, the compound showed low plasma clearance with a mean elimination half-life of 5.66 h. The V_{ss} was moderate-high, representing 1.9-fold more than the average volume of total body water. On the other hand, plasma concentrations of NPO after its oral administration at 10 mg/kg dose, were quantifiable up to 24 h with a T_{max} of 0.25 h. Calculated oral bioavailability was 47%. NPO exhibited a high plasma protein binding in mice (98.4%). The free plasma concentration at C_{max} was 1.4 μmol/L.

NPO at 10 μmol/L did not show any relevant affinity or activity when studied in a general safety *in vitro* screen panel including 44 safety-related targets. Intraperitoneal administration of NPO at doses up to 100 mg/kg/day during 4 consecutive days in male mice did not reveal any mortality and clinical sign and did not affect body weight, weight gain, feed consumption, functional observation battery, or gross pathology. Mean plasma concentrations of NPO determined at 24 h post last dosing in mice treated with 10, 30, and 100 mg/kg/day suggest a long half-life and linear dynamics (72.24, 172.52, and 579.35 ng/mL, respectively).

Cardioprotective efficacy of NPO-2270 in the *ex vivo* rat model of ischemia/reperfusion

A dose-response study was performed in Langendorff-perfused rat hearts subjected to transient ischemia. A schematic illustration of the experimental protocol is shown in Figure 1A. At the end of the equilibration period LV end-diastolic pressure (LVEDP) and LV developed pressure (LVdevP, which is LV end-systolic pressure (LVESP) – LVEDP) were 7.2 ± 0.4 and 92.7 ± 5.4 mmHg respectively, perfusion pressure was 62.5 ± 2.9 mmHg and coronary flow 11.8 ± 1.9 mL/min in the control group. No differences among groups were observed in LV function during the equilibration and the ischemic period. In control hearts, reperfusion induced an abrupt increase in LVEDP with a peak of 113 ± 6.5 mmHg 3 min after onset, severe contractile dysfunction (5% recovery of initial LVdevP value after 1 h of reperfusion), and cell death (LDH release and infarct size were 385 ± 19 U/30 min/gdw and 46.5 ± 2.1%, respectively). Addition of NPO to the perfusion buffer during reperfusion was associated with a reduction in peak LVEDP (34% of reduction in 10 μmol/L NPO group vs. control group, EC_{50} value of 52 ± 6 nmol/L) and in acute cell death, measured as LDH release and infarct size (calculated EC_{50} values of 32 ± 7 nmol/L, 61 ± 5 nmol/L, respectively) and improved ventricular function. Cardioprotection was observed at the concentration of 0.1 μmol/L and functional recovery at 1 μmol/L, with a statistically non-significant trend toward greater protection at higher doses (Figures 1B–1D). Reperfusion induced calpain activation, as denoted by a reduction in the 145/150 α-fodrin fragments, without significant changes in calpain-1 and calpain-2 protein levels (Figure 1E). NPO treatment resulted in a dose-dependent calpain inhibition, with a calculated IC_{50} value of 12 ± 3 nmol/L (Figure 1F). Regression plot analysis, including all NPO-treated groups, disclosed a close correlation between the magnitude of calpain inhibition and cardioprotection ($r^2 = 0.95$, $p < 0.001$; Figure 1G).

NPO-2270 administration immediately before reperfusion reduces infarct size *in vivo*

Based on the results obtained in our *ex vivo* model, NPO was tested in mice subjected to 45 min of coronary occlusion followed by 24 h of reperfusion at the doses of 5 and 20 mg/kg, given intraperitoneally 10 min before reperfusion onset (Figure 2A). There were no significant

Table 2. Pharmacokinetic parameters of NPO-2270 in mice following single intravenous (IV) and oral (PO) administration

Compound	Route	Dose (mg/kg)	T_{max} (h)	C_0/C_{max} [a] (ng/mL)	AUC_{last} (ng/mL*h)	AUC_{inf} (ng/mL*h)	$T_{1/2}$ (h)	CL (mL/min/kg)	Vss (L/kg)	%F[b]
NPO-2270	IV (n = 3)	1	–	2753.48	3266.31	3358.31	5.66	4.96	1.35	–
	PO (n = 3)	10	0.25	4112.90	15298.88	15391.97	–	–	–	47

[a]back extrapolated concentration for IV group.
[b]AUClast considered for calculating the bioavailability.

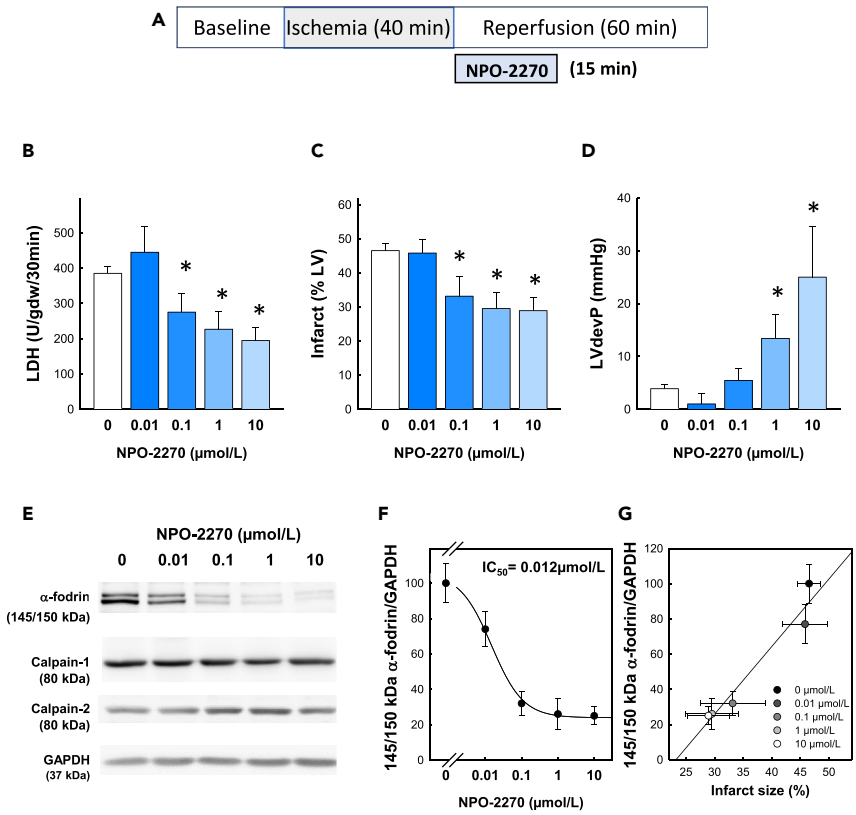

Figure 1. Dose-dependent cardioprotective effects of NPO-2270 in the *ex vivo* rat heart model

(A) Isolated rat hearts were perfused in a Langendorff system and subjected to 40 min of ischemia and 60 min of reperfusion. NPO-2270 was added during the first 15 min of reperfusion.

(B–D) Cardioprotective effects of NPO-2270 were evaluated by measuring lactate dehydrogenase (LDH) release, infarct size and LV developed pressure (LVdevP); n = 6–9 per group.

(E and F) Representative western blots and quantification of 145/150 kDa α-fodrin, calpain 1, and calpain 2 protein expression; n = 6–7 per group.

(G) Correlation between infarct size and calpain activity measured as α-fodrin cleavage; n = 6–7 per group. Results are mean ± SEM. *$p < 0.05$ vs. Control (0 µmol/L) analyzed using one-way ANOVA followed by Tukey's post-hoc test.

differences between control and NPO groups in the area of myocardium at risk, while administration of 20 mg/kg NPO reduced infarct size by 32% (32.5 ± 3.1% in the NPO group vs. 47.8 ± 4.3% in the control group, $p = 0.016$) (Figure 2B). At the dose of 5 mg/kg, NPO showed a strong trend toward protection, but it did not reach statistical significance (36.2 ± 4.2%, $p = 0.053$). By contrast, acute administration of the cathepsin inhibitor balicatib failed to attenuate infarct size (Figure 2B). At this concentration, balicatib reduced cathepsin L activity measured in heart homogenates (41.2 ± 7.3% compared to sham mice, n = 3 per group) with no significant differences with respect to mice treated with 20 mg/kg NPO (35.2 ± 6.7%; n = 3 per group). Reperfusion was associated with increased calpain activation without changes in calpain protein expression. Both, low and high dose of NPO produced a marked attenuation of α-fodrin cleavage measured after 24 h of reperfusion (47.3 ± 8.2% and 60.1 ± 6.7% respectively), confirming the efficacy of *in vivo* NPO administration in preventing calpain activation (Figure 2C).

NPO-2270 preserves cardiac function after ischemic and non-ischemic stress more effectively than enalapril

The effects of chronic oral administration of NPO on cardiac remodeling and heart function were analyzed in mice subjected to transient ischemia and transverse aortic constriction (TAC) surgery and compared to enalapril treatment.

An illustration of the experimental protocol corresponding to the ischemia/reperfusion studies is shown in Figure 3A. Baseline echocardiographic evaluation did not show any difference between groups. In control animals, myocardial infarction resulted in a progressive increase in left ventricular end-diastolic diameter (LVEDD) and LVESD and a decrease in ejection fraction (EF) that was already significant after two weeks of reperfusion (Figures 3B and 3C). No changes in left ventricular posterior wall thickness (LVPWT) and intraventricular septum thickness (IVST) were observed (Table 3). Administration of NPO at the time of reperfusion was more effective than enalapril in preventing LV dilatation and dysfunction as compared to control hearts (p = 0.003 between NPO and control group, and p = 0.072 between NPO and enalapril groups with respect to EF reduction; Figure 3C).

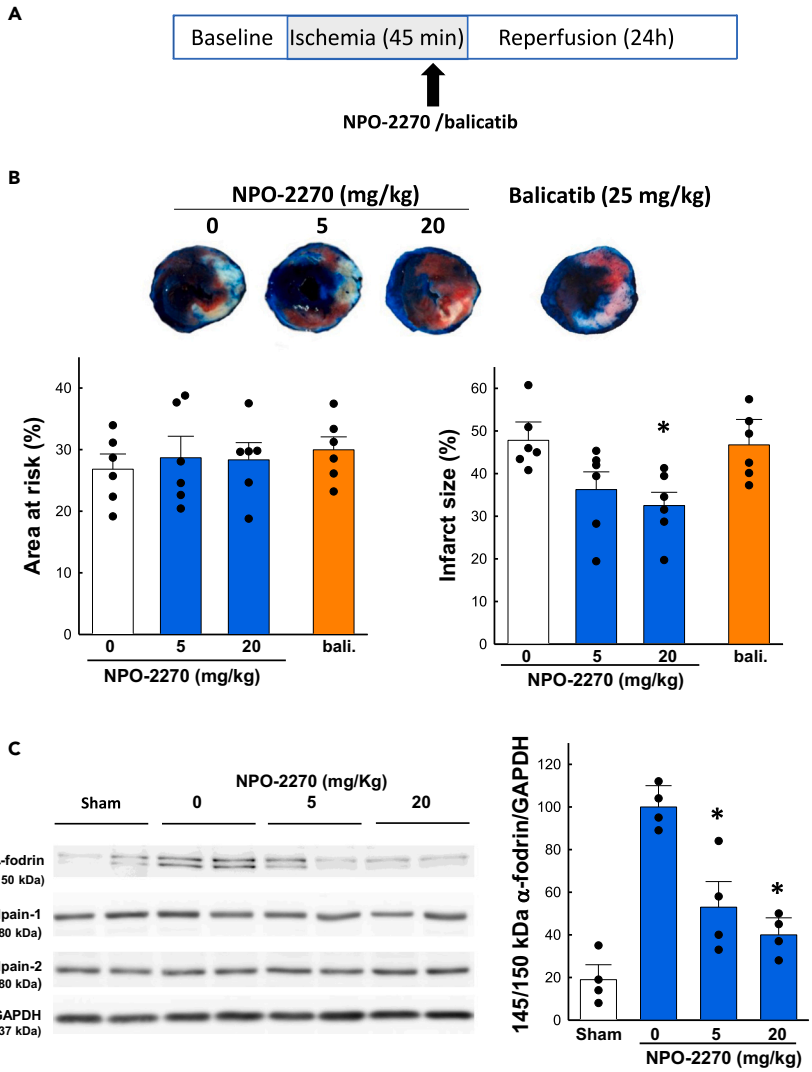

Figure 2. NPO-2270 attenuates acute reperfusion injury

(A) Mice were subjected to 45 min of coronary occlusion and 24 h of reperfusion. NPO-2270 or balicatib were intraperitoneally administrated 10 min before starting reperfusion.

(B) Representative images from transversely sectioned heart slices showing the area at risk (Evans Blue) and of necrosis (triphenyltetrazolium) and quantification of area at risk expressed as percentage of LV area and infarct size expressed as percentage of the region at risk (n = 6 per group).

(C) Representative Western blots of 145/150 kDa α-fodrin, calpain 1, and calpain 2 protein expression, and quantification of 145/150 kDa α-fodrin (n = 4 per group). Bali: balicatib. Results are mean ± SEM. *$p < 0.05$ vs. Control group analyzed using one-way ANOVA followed by Tukey's post-hoc test.

Scar size after 28 days of treatment was significantly smaller in the NPO and enalapril groups than in the control group (43% of reduction, $p < 0.001$, and 24%, $p = 0.030$ respectively), without significant differences among treatments (Figure 3D). There was not significant difference in mortality rates between groups (15% in the control group, 11% in the NPO group, and 20% in the enalapril group). Both, calpain-1 and calpain-2 were overexpressed (49% of increase, $p = 0.019$, and 75%, $p = 0.008$ respectively), and activated during late reperfusion. Chronic NPO but not enalapril treatment attenuated α-fodrin cleavage (52% of reduction vs. control group, $p < 0.001$) without decreasing calpain-1 and calpain-2 expression (Figure 3E).

To determine the most appropriate dose of NPO to use in the TAC studies we first performed dose-response studies in angiotensin II-treated mice. Daily oral administration of NPO resulted in a dose-dependent attenuation of angiotensin II-induced hypertrophy as reflected by decreased heart weight-to-tibia length ratio (HW/TL), LVPWT, IVST and brain natriuretic peptide (BNP) and Myh7 mRNA levels, and markedly attenuated interstitial fibrosis and collagen 1 and 3 mRNA levels (Figure S1; Table 1). Based on these results, TAC mice were orally treated with 10 mg/kg NPO or with enalapril at the same dose to compare the potency of NPO relative to enalapril.

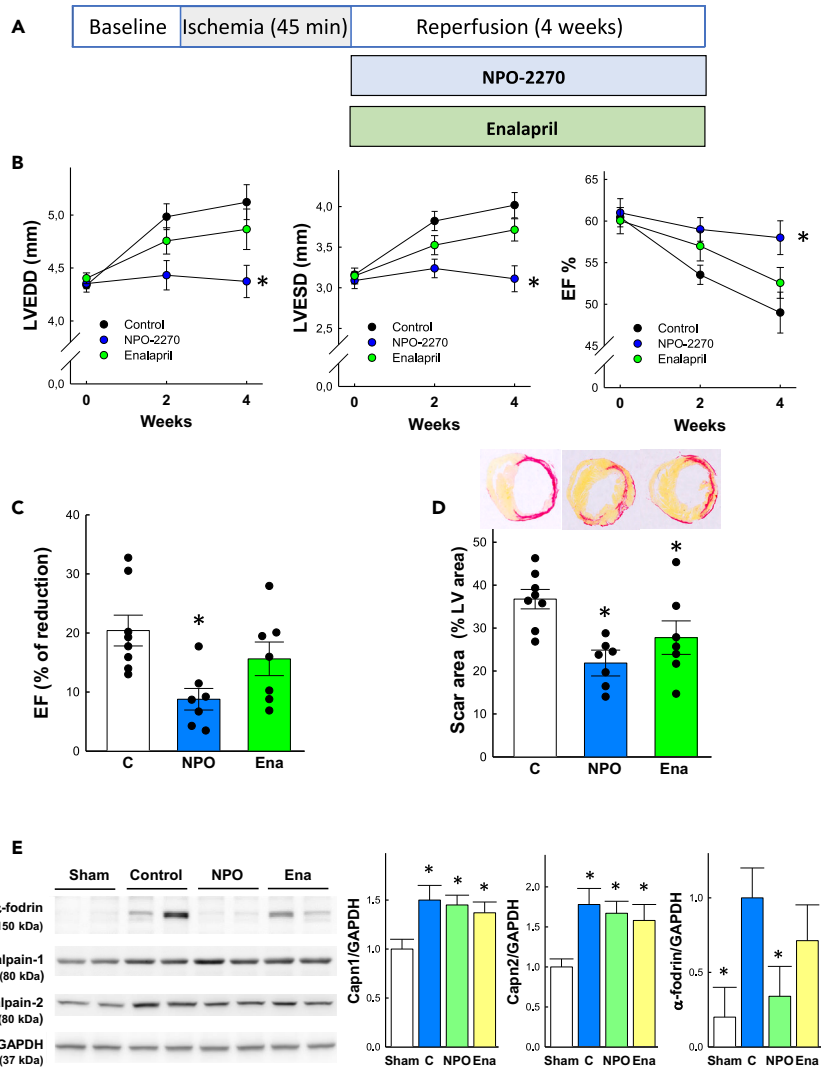

Figure 3. Chronic oral administration of NPO-2270 prevents post-infarction induced cardiac dysfunction

(A) Mice were subjected to 45 min of coronary occlusion and 28 days of reperfusion and received NPO-2270 (20 mg/kg) orally or enalapril (20 mg/kg) for 28 days.

(B) Time course of left ventricular ejection fraction (EF), left ventricular end-diastolic diameter (LVEDD), and left ventricular end-systolic diameter (LVESD) in the different experimental groups.

(C) EF reduction with respect to baseline values expressed in percentage.

(D) Representative images from transversely sectioned heart slices showing the scar area and its quantification expressed as percentage of LV area.

(E) Representative Western blots and quantification of 145/150 kDa α-fodrin, calpain 1, and calpain 2 protein expression. C: control group, NPO: NPO-2270 group, Ena: enalapril group. Results are mean ± SEM, *$p < 0.05$ vs. Control group analyzed using repeated measures ANOVA or one-way ANOVA followed by Tukey's post-hoc test; $n = 8$ in control group, $n = 7$ in NPO-2270 and enalapril groups; western-blot: $n = 4$ per group).

A schematic illustration of the different experimental groups corresponding to the TAC studies is shown in Figure 4A. Compared to control group, the chronic oral administration of NPO starting 1 week after TAC surgery prevented the progression of hypertrophy, as shown by changes in HW/TL (Figure 4B), cardiomyocyte cross-sectional area (Figure 4C), BNP mRNA levels and the Myh7-to-Myh6 ratio (Figure 4D), and LVPWT and IVST values (Table 4), and of interstitial fibrosis (Figures 4E and 4F), with no statistically significant differences with respect to the administration of enalapril for the same time interval (Figure 4; Table 4).

CD31 staining was performed in sections of mice hearts to analyze microvessel density (Figure 5A). The number of CD31-expressing cells as well as the ratio of CD31 positive cells to cardiomyocytes decreased significantly 4 weeks after TAC (43%, $p < 0.001$ and 59%, $p < 0.001$ of reduction vs. Sham group, respectively; Figure 5B). Administration of NPO or enalapril starting 1 week after TAC surgery preserved capillary density without statistically significant differences between the two treatments.

Immunohistochemistry using an antibody against CD45 revealed increased recruitment of inflammatory cells (Figure S2A), along with enhanced expression of the pro-inflammatory markers interleukin- 1β (IL-1β), IL-6, monocyte chemoattractant protein 1 (MCP-1), and tumor

Table 3. Echocardiographic data after 4 weeks of reperfusion

	Sham-operated (n = 8)	Control (n = 8)	NPO-2270 (n = 8)	Enalapril (n = 7)
BW (g)	27.3 ± 0.6	28.4 ± 0.4	27.7 ± 0.8	30.1 ± 0.9
HR (beats/min)	454 ± 26	442 ± 22	441 ± 33	461 ± 18
LVPWT (mm)	0.65 ± 0.01	0.71 ± 0.02	0.68 ± 0.03	0.67 ± 0.02
IVST (mm)	0.74 ± 0.01	0.79 ± 0.02	0.76 ± 0.03	0.79 ± 0.03
LVEDD (mm)	4.29 ± 0.07	5.07 ± 0.14$^{\$}$	4,49 ± 0.11*	4.85 ± 0.19
LVESD (mm)	3.04 ± 0.08	4.05 ± 0.15$^{\$}$	3.31 ± 0.09*	3.75 ± 0.12
FS (%)	29.1 ± 1.20	20.2 ± 1.3$^{\$}$	26.1 ± 1.3*	22.7 ± 1.3
EF (%)	62.1 ± 1.7	49.0 ± 2.6$^{\$}$	59.6 ± 1.9*	52.6 ± 2.2

BW, body weight; EF, ejection fraction; FS, fractional shortening; HR, heart rate; IVST, intraventricular septum thickness; LVEDD, left ventricular end-diastolic diameter; LVESD, left ventricular end-systolic diameter; LVPWT, left ventricular posterior wall thickness. Values are mean ± SEM. ANOVA and Tukey's post-hoc test. $^{\$}p < 0.05$ vs. Sham operated group. *$p < 0.05$ vs. Control group.

necrosis factor alpha (TNFα) after 1 week of TAC (Figure S2B). However, after 4 weeks of TAC, no statistically significant differences were observed in any of these markers compared to the sham group, although there was a trend for IL-6 and TNF-α levels to be higher in control hearts than in those treated with NPO or enalapril.

Both treatments attenuated LV dilation (Figures 6A and 6B) and EF reduction (Figure 6C) compared to control mice. However, ventricular dysfunction measured after 4 weeks of TAC surgery was significantly less severe in the NPO group than in the enalapril group (27% of EF reduction with respect to baseline in the control group, 6% in the NPO group and 16% in the enalapril group, $p = 0.024$ between NPO and enalapril groups, Figure 6; Table 4). The administration of NPO from the first day after TAC surgery or the coadministration of NPO and enalapril were not superior to NPO alone starting 1 week after TAC surgery in any measured parameter (Figures 4, 5, and 6).

Mortality occurred during the first week, and there were no differences between the control group and the group treated with NPO from the first day after surgery (30% and 28% respectively). After the first week of TAC, all mice survived, regardless of the experimental group.

In further experiments, it was assessed whether NPO administration prevents the progression of pre-existing HF. In C57BL/6N mice subjected to pressure overload, the echocardiographic results obtained two weeks after TAC surgery demonstrated ventricular remodeling and dysfunction (32% reduction in EF compared to baseline in the control group, $p < 0.001$). Oral administration of NPO during the following 3 weeks significantly attenuated the progression of adverse ventricular remodeling, as measured by changes in the HW/TL ratio, LVPWT, IVST and ventricular dilation, and cardiac dysfunction compared to the control group (29% vs. 5% EF reduction in the control and NPO groups during the 3 weeks of treatment, respectively, $p = 0.003$) but did not regress the alterations already established at the onset of the treatment (Table S2).

NPO-2270 preserves junctophilin-2 striated pattern

Western blot results confirmed that calpain-1 and calpain-2 are overexpressed and activated after TAC surgery (Figure 7A). The measurement of fodrin cleavage products indicates that calpain activity was markedly attenuated in mice treated with NPO but not with enalapril, and no additive effect was observed after the coadministration of both drugs. Neither NPO nor enalapril modified calpain expression.

Junctophilin-2 (JP2) is a structural protein essential for organizing the ultrastructural machinery, i.e., cardiac dyads, required for normal excitation-contraction coupling function and Ca^{2+} handling in cardiomyocytes. In healthy ventricular cardiomyocytes, JP2 is localized in a striated pattern along the well-arrayed Z-disc area (Figure 7B).[22,23]

As showed by western blot, and consistent with previous findings,[9] TAC-induced stress resulted in a marked decrease in the full-length JP2 and an increase in the 75 kDa JP2 N-terminal cleavage product/full-length JP2 ratio. In line with these results, confocal analysis showed a marked loss and disorganization of the JP2 striated pattern and changes in peak intensity and the variation coefficient (VC), indicative of ultrastructural damage to the cardiac dyad. In correlation with calpain activity results, NPO but not enalapril treatment prevented JP2 downregulation and the severe disorganization of the JP2 pattern observed in control hearts.

DISCUSSION

The present study characterizes NPO as a cysteine protease inhibitor with an *in vitro* potency in the nanomolar range and good oral bioavailability. We first established that acute administration of NPO in rodent models of transient ischemia at the time of reperfusion reduces myocardial infarction in association with calpain inhibition, while its chronic oral administration attenuates LV dilatation and dysfunction induced by ischemic and non-ischemic pathological stimuli. Then, our study compared the efficacy of cysteine protease inhibition with a conventional treatment of patients with LV dysfunction or HF and demonstrated that NPO attenuates cardiac dysfunction more effectively than enalapril when given at the same dose. Finally, we provide evidence showing that the effects of NPO correlate

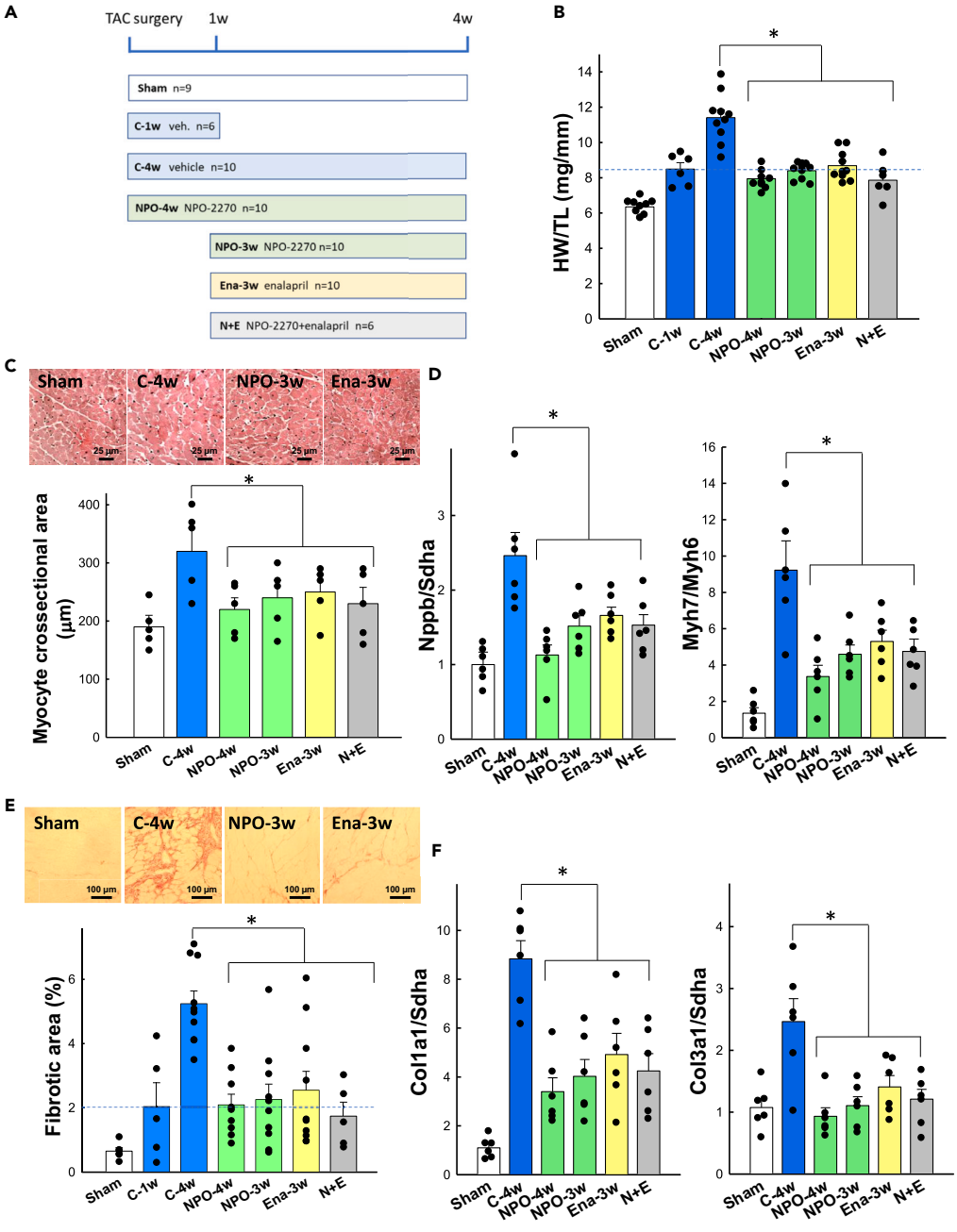

Figure 4. NPO-2270 prevents ventricular remodeling progression in TAC mice

(A) NPO-2270 was administered orally at the time of TAC surgery or one week after. Enalapril or the combination of both drugs were administered one week after TAC surgery.

(B) Heart weight/tibia length ratio (n = 9 in sham group; n = 6 in C-1w and N + E groups; n = 10 in C-4w, NPO-3w and Ena-3w groups; n = 8 in NPO-4w group).

(C) Representative images corresponding to ventricular cross-sections stained with hematoxylin and eosin and quantification of cardiomyocyte cross-sectional area (n = 5 per group). Images are shown at ×400 magnification (scale, 25 μm).

(D) mRNA levels of BNP and β-myosin heavy chain normalized respect to sham group (n = 6 per group).

(E) Representative images of ventricular cross-sections stained with picrosirius red and quantification of the fibrotic area. Images are shown at ×200 magnification (scale = 100 μm) (n = 6 in sham group; n = 5 in C-1w and N + E groups; n = 10 in C-4w, NPO-3w, and Ena-3w groups; n = 9 in NPO-4w group).

(F) mRNA levels of collagen I and collagen III normalized respect to sham group (n = 6 per group). Results are mean ± SEM, *p < 0.05 vs. Control group analyzed using one-way ANOVA followed by Tukey's post-hoc test.

Table 4. Echocardiographic data at 4 weeks following TAC surgery

	Sham (n = 8)	C-4w (n = 10)	NPO-4w (n = 9)	NPO-3w (n = 10)	Ena-3w (n = 10)	N + E (n = 6)
BW (g)	27.9 ± 0.7	27.2 ± 0.7	27.5 ± 0.4	28.1 ± 0.5	27.0 ± 0.6	27.4 ± 0.6
HW (mg)	112.5 ± 2.6	200.7 ± 7.4	142.5 ± 3.9	149.9 ± 3.3	151.8 ± 4.9	140.5 ± 6.2
HW/TL (mg/mm)	6.35 ± 0.14	11.41 ± 0.44$^{\$}$	7.90 ± 0.18$^{\$*}$	8.40 ± 0.15$^{\$*}$	8.68 ± 0.26$^{\$*}$	7.86 ± 0.50$^{\$*}$
HR (beats/min)	475 ± 11	488 ± 18	461 ± 22	466 ± 19	479 ± 15	480 ± 21
LVPWT (mm)	0.62 ± 0.02	0.83 ± 0.03$^{\$}$	0.74 ± 0.01$^{\$*}$	0.75 ± 0.02$^{\$*}$	0.78 ± 0.03$^{\$}$	0.75 ± 0.02$^{\$*}$
IVST (mm)	0.74 ± 0.01	1.08 ± 0.04$^{\$}$	0.84 ± 0.02$^{\$*}$	0.9 ± 0.02$^{\$*}$	0.97 ± 0.03$^{\$*}$	0.88 ± 0.03$^{\$*}$
LVEDD (mm)	4.22 ± 0.10	4.91 ± 0.06$^{\$}$	4.22 ± 0.10*	4.26 ± 0.14*	4.48 ± 0.05*	4.31 ± 0.26*
LVESD (mm)	3.01 ± 0.04	4.02 ± 0.10	3.26 ± 0.13$^{\$}$	3.27 ± 0.09*	3.55 ± 0.05$^{\$*}$	3.02* ± 0.33
FS (%)	26.8 ± 1.3	18.3 ± 1.06$^{\$}$	24.2 ± 1.4*	23.4 ± 1.1*	20.8 ± 0.8$^{\$*}$	25.1 ± 2.1*
EF (%)	58.9 ± 0.7	42.6 ± 1.8$^{\$}$	54.7 ± 1.8*	54.3 ± 1.9*	49.5 ± 1.6$^{\$*}$	55.8 ± 1.4*

BW, body weight; EF, ejection fraction; FS, fractional shortening; HR, heart rate; IVST, intraventricular septum thickness; LVEDD, left ventricular end-diastolic diameter; LVESD, left ventricular end-systolic diameter; LVPWT, left ventricular posterior wall thickness. Values are mean ± SEM. ANOVA and Tukey's post-hoc test. $^{\$}p < 0.05$ vs. Sham operated group. $^{*}p < 0.05$ vs. Control group.

with calpain inhibition and the preservation of the T-tubule morphology due at least in part to reduced cleavage of the calpain substrate JP2.

Compelling experimental evidence obtained in multiple HF models points to calpain inhibition as a potential therapeutic strategy to reduce adverse myocardial remodeling and dysfunction.[15,16] Despite this solid evidence, no clinical trials and only a few preclinical studies have explored the pharmacological inhibition of calpains as a therapeutic opportunity for HF. In previous studies, chronic intraperitoneal administration of MDL-28170 and oral administration of SNJ-1945 reduced adverse cardiac remodeling and HF induced by ischemic and non-ischemic stimuli.[6,8,24] However, the pharmacokinetics and poor bioavailability of MDL-28170 and the low potency for SNJ-1945 have precluded their use in clinical studies. In addition, although these studies are important proof of concept, preclinical validation requires a head-to-head comparison of the efficacy of calpain inhibition with standard pharmacological HF treatment. These issues were addressed in this study.

Herein, we have characterized NPO as a highly selective cysteine protease inhibitor with *in vitro* potency in the nanomolar range not only for calpain-1 and calpain-2 but also for relevant cathepsins. Pharmacokinetic data indicate that NPO is rapidly absorbed by the oral route and has a long half-life in rodents and support that the achieved free plasma concentrations are compatible with its protease inhibitory activity. Perfusion of isolated rat hearts with NPO at the onset of reperfusion attenuated cell death in close correlation with the magnitude of calpain inhibition and its acute administration during the last minutes of ischemia, but not of a cathepsin inhibitor, reduced infarct size and calpain activity in an *in vivo* mouse model of transient coronary occlusion. These results provide evidence for the rapid penetration of NPO, confirm that its potency *in vivo* against calpains is in the nanomolar range, and are in agreement with the important contribution of calpains to reperfusion injury.[25] In addition, although limited, the favorable safety and toxicological data strongly suggest a wide safety window.

Daily oral administration of NPO after 1 week of TAC surgery abrogated the progression of myocardial hypertrophy and fibrosis, with no significant differences with respect to enalapril treatment given at the same concentration but attenuating the ongoing cardiac dysfunction more effectively. Furthermore, the greater efficacy of NPO in preventing cardiac dysfunction was also confirmed in the post-infarcted heart model. Importantly, NPO effects correlated with the inhibition of calpain activity as demonstrated by the reduced cleavage of the calpain substrate α-fodrin observed in both experimental models. The administration of NPO from the first day after TAC surgery was not more effective than its administration after 1 week, which is in agreement with an enhanced calpain activity due to a progressive increase in protein expression.

Moreover, administration of NPO to TAC mice with stablished ventricular dysfunction prevented further progression of adverse remodeling and HF, although without reversing the echocardiographic alterations observed at the initiation of the treatment. Additional experiments would be necessary to determine if long-term NPO treatment can regress adverse ventricular remodeling.

We have previously described that oral administration of the calpain inhibitor SNJ-1945 attenuate post-infarction remodeling induced by transient ischemia,[8] as well as hypertrophy triggered by chronic administration of isoproterenol.[24] However, it is important to note that while the low potency of SNJ-1945 limits its translation to patients, the effects of NPO have been achieved at doses that are potentially translatable to clinical practice.

In our experimental conditions, where NPO and enalapril were compared at the same dose, NPO or the combination of NPO and enalapril was superior to the administration of enalapril alone. This observation is consistent with studies suggesting that the overexpression and overactivation of calpains represent a convergence point for a variety of receptors and signaling pathways activated by chronic pathological stimuli. Supporting this concept, our current data and previous findings indicate that calpains drive myocardial remodeling induced by chronic angiotensin administration,[26] as well as that caused by the activation of beta-adrenergic receptors,[24] mechanoreceptors,[27] and TGF-β.[8]

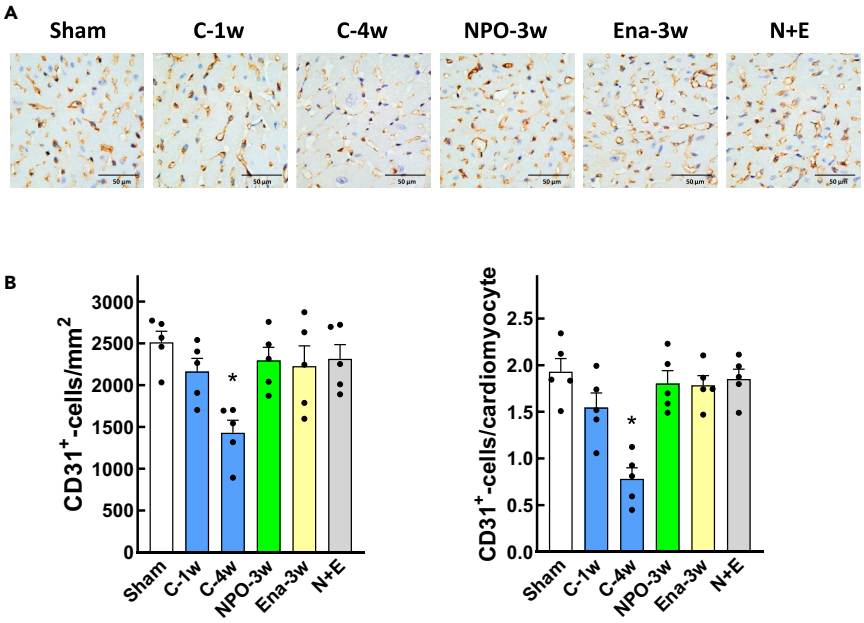

Figure 5. NPO-2270 preserves microvascular density in TAC mice

(A) Representative images corresponding to ventricular cross-sections immunostained against CD31.

(B) Quantification of $CD31^+$ cells per area and ratio of $CD31^+$ cells to cardiomyocytes. Images are shown at ×400 magnification (scale = 50 μm). Data are presented as mean ± SEM. *$p < 0.05$ vs. Sham group analyzed using one-way ANOVA followed by Tukey's post-hoc test; $n = 5$ per group.

According to these studies, it seems reasonable to expect a more potent effect through direct inhibition of calpains rather than inhibiting only one of the pathways causing such activation.

Previous studies have characterized many proteins with important roles in maintaining cardiac function as calpain substrates.[28] Among them, JP2 plays a critical role in maintaining T-tubule anchored to the sarcoplasmic reticulum to allow the control of calcium fluxes for an effective contractile function.[29,30] Cardiac specific deletion of JP2 causes T-tubule disruption, severe impairment of intracellular Ca^{2+} handling, and heart failure in mice[30,31] while its transgenic and virally mediated overexpression attenuates LV dysfunction induced by TAC surgery.[32,33] The calpain-dependent cleavage of JP2 has been causally associated with T-tubule disorganization and HF development in preclinical models,[29] and increased calpain activity correlated with loss of JP2 expression in human failing hearts.[6] Herein, our results show that the greater effect of NPO versus enalapril on cardiac function observed in TAC mice was associated with an effective inhibition of calpain activity, reduced JP2 cleavage and better preservation of the JP2 striated pattern. Since calpain-dependent degradation of JP2, and its contribution to cardiac dysfunction, has also been described in post-infarction remodeling,[6] it is expected that the effect of NPO on JP2 degradation in our ischemia/reperfusion model will be similar to that observed in the TAC model. Nevertheless, our results do not exclude the contribution of additional mechanisms related to the proteolysis of other cysteine protease substrates.[15,16]

Classically, calpain inhibitors have shown poor target selectivity over cysteine proteases cathepsins. In fact, the compounds previously used in preclinical models of HF, MDL-28170 and SNJ-1945, inhibit at least cathepsins B and L.[34,35] This reduced selectivity against cathepsins shown in *in vitro* assays has been considered an obstacle to their therapeutic progression. However, some evidence may question whether the design of pure specific calpain inhibitors is the best strategy for the achievement of optimal clinical results. Increased expression and activity of cathepsins have been described in patients with HF, and they inversely correlated with clinical outcomes,[36,37] and the use of knockout mice provides evidence for the contribution of the cysteine cathepsins K, B, L, and S to the development of adverse cardiac remodeling and contractile dysfunction, although ambiguous in chronic ischemia.[38] There is also evidence suggesting that calpain overactivation increases lysosomal permeability and produces the release of cathepsins to the cytosol where they may contribute to neuronal injury (calpain-cathepsin hypothesis).[39] Although this hypothesis needs to be confirmed in the context of cardiac remodeling, the pharmacological inhibition of both calpain and cathepsins seems a reasonable approach.[40]

Conclusions

In conclusion, NPO appears as a potent and selective cysteine protease inhibitor. Its robust efficacy in preventing the progression of cardiac remodeling and reducing cardiac dysfunction compared with enalapril in various rodent models of HF supports continuing its development in further clinically relevant models as a previous step for its clinical evaluation in patients.

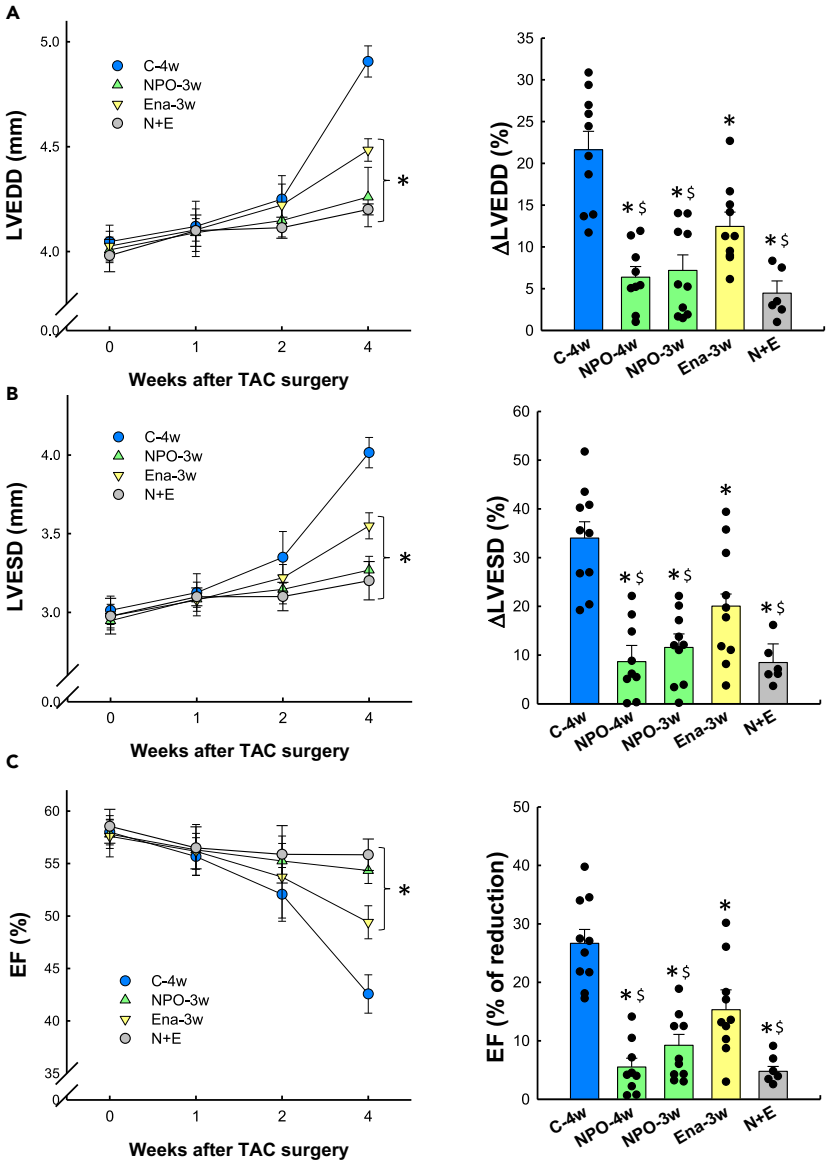

Figure 6. NPO-2270 preserves cardiac function in TAC mice more effectively than enalapril

(A–C) Time course and percentage of variation with respect to baseline values of: (A) left ventricular end-diastolic diameter (LVEDD), (B) left ventricular end-systolic diameter (LVESD), and (C) left ventricular ejection fraction (EF) in control mice and mice receiving NPO-2270 or enalapril after 1 week of TAC surgery. Results are mean ± SEM, *$p < 0.05$ vs. Control group (C-4w). $^{\$}p < 0.05$ vs. enalapril group (Ena-3w) analyzed using repeated measures ANOVA or one-way ANOVA followed by Tukey's post-hoc test; $n = 10$ in C-4w, NPO-3w, and Ena-3w groups; $n = 9$ in NPO-4w group; $n = 6$ in N + E group.

Limitations of the study

The administration of balicatib at a concentration that was effective in reducing cathepsin activity failed to attenuate infarct size, supporting a predominant deleterious role of calpains over cathepsins during the acute phase of reperfusion. However, although our results show NPO as a potent orally active calpain inhibitor, and its effects on cardiac remodeling and HF correlate with calpain inhibition, we recognize that further preclinical investigation is necessary to determine the relative contribution of those cathepsins inhibited by NPO *in vitro*. By administering both treatments at the same dose, our results compare the potency of NPO to that of enalapril. The selected dose of enalapril, which has been used in previous studies,[20,21,41] effectively prevented the progression of adverse ventricular remodeling in our study (Figures 4B and 4E). However, since we did not conduct a dose-response study to determine the maximum effective enalapril dose, we cannot rule out the possibility of an additional benefit at higher doses. Finally, although calpain overexpression has been described in heart samples from both men and women with heart failure,[5] and the contribution of calpains to adverse cardiac remodeling has been described in mice from both sexes,[42] the animals used in this study were male, and females may exhibit different drug responses.

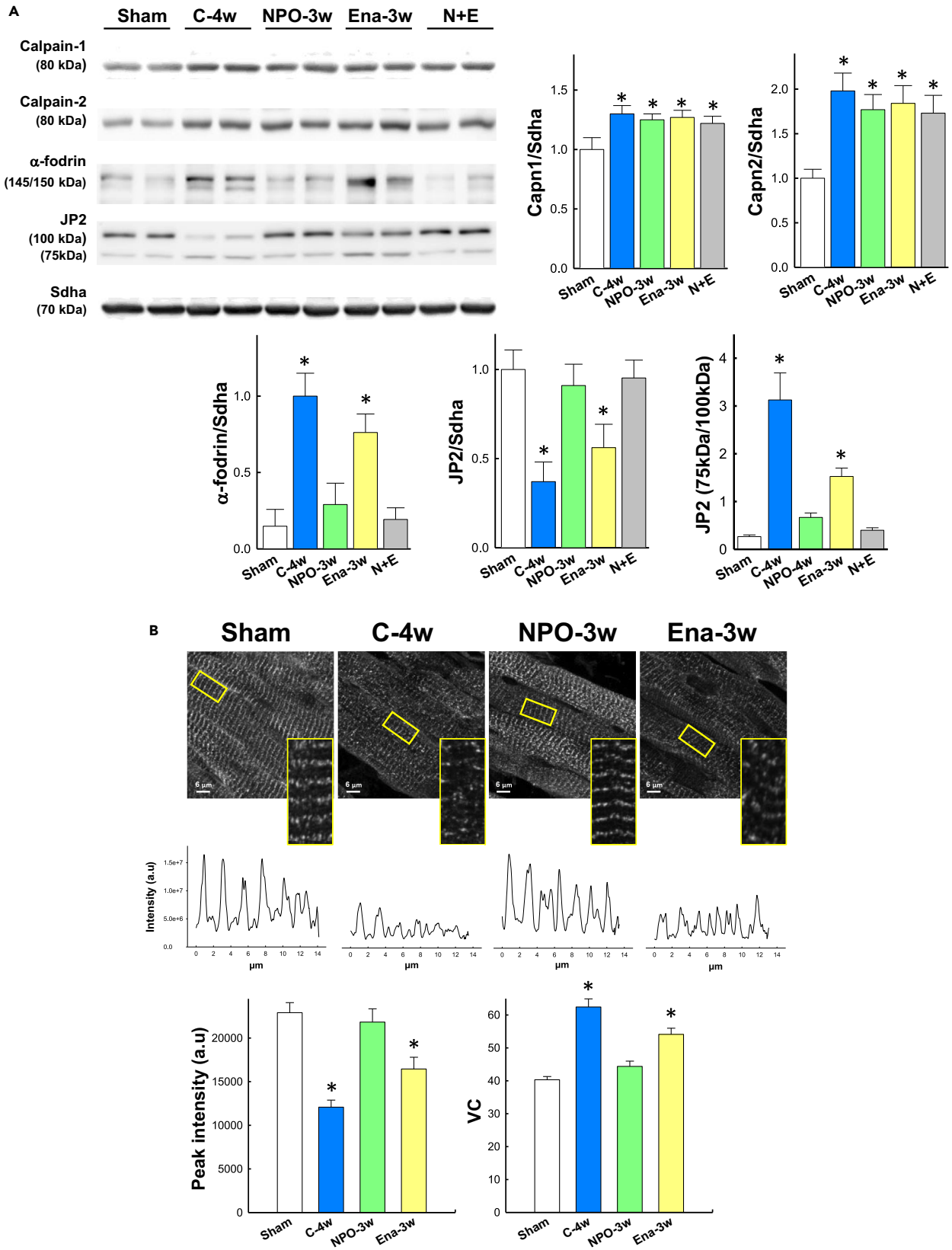
A
Sham
C-4w
NPO-3w
Ena-3w
N+E
Calpain-1
(80 kDa)
Calpain-2
(80 kDa)
α-fodrin
(145/150 kDa)
JP2
(100 kDa)
(75kDa)
Sdha
(70 kDa)
Capn1/Sdha
Capn2/Sdha
α-fodrin/Sdha
JP2/Sdha
JP2 (75kDa/100kDa)
B
Sham
C-4w
NPO-3w
Ena-3w
6 μm
Intensity (a.u)
μm
Peak intensity (a.u)
VC

Figure 7. NPO-2270 inhibits calpain and preserves junctophilin-2 striated pattern

(A) Representative western blots and quantification of calpain 1, calpain 2, 145/150 kDa α-fodrin, full-length JP2 protein expression and 75 kDa JP2 cleavage product normalized to full length JP2, in ventricular samples obtained after 4 weeks of TAC surgery ($n = 6$ per group).

(B) Representative processed confocal images of left ventricle sections stained for JPH2. Profile analysis of the magnified insets and quantification of peak intensities and variation coefficient (VC) ($n = 6$–8 cells from 3 hearts per group). Results are mean ± SEM. *$p < 0.05$ vs. sham group analyzed using one-way ANOVA followed by Tukey's post-hoc test.

RESOURCE AVAILABILITY

Lead contact

Further information and requests should be directed to and will be fulfilled by the lead contact, Dr. Javier Inserte (javier.inserte@vhir.org).

Materials availability

Materials generated in this study are available upon reasonable request from the lead contact.

Data and code availability

- All data reported in this paper will be shared by the lead contact up on request.
- This paper does not report original code.
- Any additional information required to reanalyze the data reported in this paper is available from the lead contact upon request.

ACKNOWLEDGMENTS

This work was funded by Instituto de Salud Carlos III, Spain, through the projects AES PI20/01681 and AES PI23/00068; and the research network CIBERCV (CB16/11/00479), both cofunded by European Regional Development Fund; Sociedad Española de Cardiología (SEC/FEC-INV-BAS 22/013); Fundació la Marató de TV3 (FLMTV3/202321-30-31) and PERIS STL/484/2023. Long-Sheng Song is supported by the National Institutes of Health of USA.

AUTHOR CONTRIBUTIONS

D.A.: investigation, methodology, formal analysis, writing – original draft. S.D.T.: investigation. J.A.B.: conceptualization, funding acquisition. E.M.C.: investigation. M.R.M.: writing – review and editing. A.R.S.: writing – review and editing. B.B.: writing – review and editing. J.W.: investigation and methodology. L.S.S.: investigation and methodology. I.F.G.: writing – review and editing, project administration. J.I.: conceptualization, supervision, funding acquisition, writing – original draft.

DECLARATION OF INTERESTS

Dr. J. Inserte received a grant from Landsteiner Genmed SL.

STAR★METHODS

Detailed methods are provided in the online version of this paper and include the following:

- KEY RESOURCES TABLE
- EXPERIMENTAL MODEL AND STUDY PARTICIPANT DETAILS
  - Cell line
  - Animals
  - *Ex vivo* model of ischemia/reperfusion
  - *In vivo* models of acute reperfusion injury and post-infarction remodeling
  - Angiotensin II treatment
  - Transverse aortic constriction
- METHOD DETAILS
  - Cysteine protease inhibition assays
  - Pharmacokinetic properties of NPO-2270
  - Preliminary safety and toxicology studies
  - Echocardiography
  - Histology, immunohistochemistry, western blot and RT-PCR
  - Imaging of junctophilin-2
- QUANTIFICATION AND STATISTICAL ANALYSIS

SUPPLEMENTAL INFORMATION

Supplemental information can be found online at https://doi.org/10.1016/j.isci.2024.110935.

Received: April 23, 2024
Revised: July 29, 2024
Accepted: September 9, 2024
Published: September 11, 2024

REFERENCES

1. Riccardi, M., Sammartino, A.M., Piepoli, M., Adamo, M., Pagnesi, M., Rosano, G., Metra, M., von Haehling, S., and Tomasoni, D. (2022). Heart failure: an update from the last years and a look at the near future. ESC Heart Fail. *9*, 3667–3693.
2. Goll, D.E., Thompson, V.F., Li, H., Wei, W., and Cong, J. (2003). The calpain system. Physiol. Rev. *83*, 731–801.
3. Inserte, J. (2012). Calpains in the cardiovascular system. Cardiovas. Res. *96*, 9.
4. Penela, P., Inserte, J., Ramos, P., Rodriguez-Sinovas, A., Garcia-Dorado, D., and Mayor, F., Jr. (2019). Degradation of GRK2 and AKT is an early and detrimental event in myocardial ischemia/reperfusion. EBioMedicine *48*, 605–618.
5. Yang, D., Ma, S., Tan, Y., Li, D., Tang, B., Zhang, X., Sun, M., and Yang, Y. (2010). Increased expression of calpain and elevated activity of calcineurin in the myocardium of patients with congestive heart failure. Int. J. Mol. Med. *26*, 159–164.
6. Wang, Y., Chen, B., Huang, C.K., Guo, A., Wu, J., Zhang, X., Chen, R., Chen, C., Kutschke, W., Weiss, R.M., et al. (2018). Targeting Calpain for Heart Failure Therapy: Implications From Multiple Murine Models. JACC. Basic Transl. Sci. *3*, 503–517.
7. Zhang, K., Cremers, M.M., Wiedemann, S., Poitz, D.M., Pfluecke, C., Heinzel, F.R., Pieske, B., Adams, V., Schauer, A., Winzer, R., et al. (2021). Spatio-temporal regulation of calpain activity after experimental myocardial infarction in vivo. Biochem. Biophys. Rep. *28*, 101162.
8. Poncelas, M., Inserte, J., Aluja, D., Hernando, V., Vilardosa, U., and Garcia-Dorado, D. (2017). Delayed, oral pharmacological inhibition of calpains attenuates adverse post-infarction remodelling. Cardiovasc. Res. *113*, 950–961.
9. Wang, J., Ciampa, G., Zheng, D., Shi, Q., Chen, B., Abel, E.D., Peng, T., Hall, D.D., and Song, L.-S. (2021). Calpain-2 specifically cleaves Junctophilin-2 at the same site as Calpain-1 but with less efficacy. Biochem. J. *478*, 3539–3553.
10. Ye, T., Wang, Q., Zhang, Y., Song, X., Yang, D., Li, D., Li, D., Su, L., Yang, Y., and Ma, S. (2015). Over-expression of calpastatin inhibits calpain activation and attenuates post-infarction myocardial remodeling. PLoS One *10*, e0120178.
11. Kudo-Sakamoto, Y., Akazawa, H., Ito, K., Takano, J., Yano, M., Yabumoto, C., Naito, A.T., Oka, T., Lee, J.K., Sakata, Y., et al. (2014). Calpain-dependent Cleavage of N-cadherin Is Involved in the Progression of Post-myocardial Infarction Remodeling. J. Biol. Chem. *289*, 19408–19419.
12. Li, Y., Ma, J., Zhu, H., Singh, M., Hill, D., Greer, P.A., Arnold, J.M., Abel, E.D., and Peng, T. (2011). Targeted inhibition of calpain reduces myocardial hypertrophy and fibrosis in mouse models of type 1 diabetes. Diabetes *60*, 2985–2994.
13. Ma, J., Wei, M., Wang, Q., Li, J., Wang, H., Liu, W., Lacefield, J.C., Greer, P.A., Karmazyn, M., Fan, G.C., and Peng, T. (2012). Deficiency of Capn4 Gene Inhibits Nuclear Factor-κB (NF-κB) Protein Signaling/Inflammation and Reduces Remodeling after Myocardial Infarction. J. Biol. Chem. *287*, 27480–27489.
14. Ma, W., Han, W., Greer, P.A., Tuder, R.M., Toque, H.A., Wang, K.K.W., Caldwell, R.W., and Su, Y. (2011). Calpain mediates pulmonary vascular remodeling in rodent models of pulmonary hypertension, and its inhibition attenuates pathologic features of disease. J. Clin. Invest. *121*, 4548–4566.
15. Aluja, D., Delgado-Tomás, S., Ruiz-Meana, M., Barrabés, J.A., and Inserte, J. (2022). Calpains as Potential Therapeutic Targets for Myocardial Hypertrophy. Int. J. Mol. Sci. *23*, 4103.
16. Letavernier, E., Zafrani, L., Perez, J., Letavernier, B., Haymann, J.-P., and Baud, L. (2012). The role of calpains in myocardial remodelling and heart failure. Cardiovasc. Res. *96*, 38–45.
17. Llenas Calvo, J., Royo Expósito, M., Elezcano Donaire, U., Vázquez Tatay, E., Melgarejo Díaz, M., Barranco, G.M., and Medina Fuentes, E.M. (2022). Dipeptidyl Ketoamide Meta-Methoxyphenyl Derivatives and Uses Thereof. WO-2019211434-A1.2019.
18. Heidenreich, P.A., Bozkurt, B., Aguilar, D., Allen, L.A., Byun, J.J., Colvin, M.M., Deswal, A., Drazner, M.H., Dunlay, S.M., Evers, L.R., et al. (2022). AHA/ACC/HFSA Guideline for the Management of Heart Failure: A Report of the American College of Cardiology/American Heart Association Joint Committee on Clinical Practice Guidelines. J. Am. Coll. Cardiol. *79*, e263–e421.
19. McMurray, J.J.V., Packer, M., Desai, A.S., Gong, J., Lefkowitz, M.P., Rizkala, A.R., Rouleau, J.L., Shi, V.C., Solomon, S.D., Swedberg, K., et al. (2014). Angiotensin-neprilysin inhibition versus enalapril in heart failure. N. Engl. J. Med. *371*, 993–1004.
20. Mohammed, S.A., Paramesha, B., Meghwani, H., Kumar Reddy, M.P., Arava, S.K., and Banerjee, S.K. (2021). Allyl Methyl Sulfide Preserved Pressure Overload-Induced Heart Failure Via Modulation of Mitochondrial Function. Biomed. Pharmacother. *138*, 111316.
21. Qiu, X., Ma, J., Shi, Y., Zhang, D., Li, D., Dong, Z., Lin, X., Shi, H., Jiang, G., Wang, Y., and Liu, G. (2019). BAOXIN Granules Protected Mouse Model With Elevated Afterload From Cardiac Hypertrophy by Suppressing Both Inflammatory Reaction and Collagen Deposition. Front. Physiol. *10*, 820.
22. Zhang, C., Chen, B., Guo, A., Zhu, Y., Miller, J.D., Gao, S., Yuan, C., Kutschke, W., Zimmerman, K., Weiss, R.M., et al. (2014). Microtubule-mediated defects in junctophilin-2 trafficking contribute to myocyte transverse-tubule remodeling and Ca2+ handling dysfunction in heart failure. Circulation *129*, 1742–1750.
23. Guo, A., Wang, Y., Chen, B., Wang, Y., Yuan, J., Zhang, L., Hall, D., Wu, J., Shi, Y., Zhu, Q., et al. (2018). E-C coupling structural protein junctophilin-2 encodes a stress- adaptive transcription regulator. Science *362*, 1–24.
24. Aluja, D., Inserte, J., Penela, P., Ramos, P., Ribas, C., Iñiguez, M.Á., Mayor, F., Jr., and Garcia-Dorado, D. (2019). Calpains mediate isoproterenol-induced hypertrophy through modulation of GRK2. Basic Res. Cardiol. *114*, 21.
25. Hernando, V., Inserte, J., Sartório, C.L., Parra, V.M., Poncelas-Nozal, M., and Garcia-Dorado, D. (2010). Calpain translocation and activation as pharmacological targets during myocardial ischemia/reperfusion. J. Mol. Cell. Cardiol. *49*, 271–279.
26. Letavernier, E., Perez, J., Bellocq, A., Mesnard, L., de Castro Keller, A., Haymann, J.-P., and Baud, L. (2008). Targeting the calpain/calpastatin system as a new strategy to prevent cardiovascular remodeling in angiotensin II-induced hypertension. Circ. Res. *102*, 720–728.
27. Zhang, Y., Su, S.-A., Li, W., Ma, Y., Shen, J., Wang, Y., Shen, Y., Chen, J., Ji, Y., Xie, Y., et al. (2021). Piezo1-Mediated Mechanotransduction Promotes Cardiac Hypertrophy by Impairing Calcium Homeostasis to Activate Calpain/Calcineurin Signaling. Hypertension *78*, 647–660.
28. Patterson, C., Portbury, A.L., Schisler, J.C., and Willis, M.S. (2011). Tear me down: role of calpain in the development of cardiac ventricular hypertrophy. Circ. Res. *109*, 453–462.
29. Wu, C.Y.C., Chen, B., Jiang, Y.P., Jia, Z., Martin, D.W., Liu, S., Entcheva, E., Song, L.S., and Lin, R.Z. (2014). Calpain-dependent Cleavage of Junctophilin-2 and T-tubule Remodeling in a Mouse Model of Reversible Heart Failure. J. Am. Heart Assoc. *3*, 1–18.
30. Chen, B., Guo, A., Zhang, C., Chen, R., Zhu, Y., Hong, J., Kutschke, W., Zimmerman, K., Weiss, R.M., Zingman, L., et al. (2013). Critical roles of junctophilin-2 in T-tubule and excitation-contraction coupling maturation during postnatal development. Cardiovasc. Res. *100*, 54–62.
31. van Oort, R.J., Garbino, A., Wang, W., Dixit, S.S., Landstrom, A.P., Gaur, N., De Almeida, A.C., Skapura, D.G., Rudy, Y., Burns, A.R., et al. (2011). Disrupted junctional membrane complexes and hyperactive ryanodine receptors after acute junctophilin knockdown in mice. Circulation *123*, 979–988.
32. Reynolds, J.O., Quick, A.P., Wang, Q., Beavers, D.L., Philippen, L.E., Showell, J., Barreto-Torres, G., Thuerauf, D.J., Doroudgar, S., Glembotski, C.C., and Wehrens, X.H.T. (2016). Junctophilin-2 gene therapy rescues heart failure by normalizing RyR2-mediated Ca(2+) release. Int. J. Cardiol. *225*, 371–380.
33. Guo, A., Zhang, X., Iyer, V.R., Chen, B., Zhang, C., Kutschke, W.J., Weiss, R.M., Franzini-Armstrong, C., and Song, L.S. (2014). Overexpression of junctophilin-2 does not enhance baseline function but attenuates heart failure development after cardiac stress. Proc. Natl. Acad. Sci. USA *111*, 12240–12245.
34. Yoshikawa, Y., Zhang, G.X., Obata, K., Ohga, Y., Matsuyoshi, H., Taniguchi, S., and Takaki, M. (2010). Cardioprotective effects of a novel calpain inhibitor SNJ-1945 for reperfusion injury after cardioplegic cardiac arrest. Am. J. Physiol. Heart Circ. Physiol. *298*, H643–H651.
35. Simmons, G., Gosalia, D.N., Rennekamp, A.J., Reeves, J.D., Diamond, S.L., and Bates, P. (2005). Inhibitors of cathepsin L prevent severe acute respiratory syndrome coronavirus entry. Proc. Natl. Acad. Sci. USA *102*, 11876–11881.
36. Wuopio, J., Hilden, J., Bring, C., Kastrup, J., Sajadieh, A., Jensen, G.B., Kjøller, E., Kolmos, H.J., Larsson, A., Jakobsen, J.C., et al. (2018). Cathepsin B and S as markers for cardiovascular risk and all-cause mortality in patients with stable coronary heart disease during 10 years: a CLARICOR trial sub-study. Atherosclerosis *278*, 97–102.
37. Mehra, S., Kumar, M., Manchanda, M., Singh, R., Thakur, B., Rani, N., Arava, S., Narang, R., Arya, D.S., and Chauhan, S.S. (2017). Clinical significance of cathepsin L and cathepsin B in

dilated cardiomyopathy. Mol. Cell. Biochem. *428*, 139–147.

38. O'Toole, D., Zaeri, A.A.I., Nicklin, S.A., French, A.T., Loughrey, C.M., and Martin, T.P. (2020). Signalling pathways linking cysteine cathepsins to adverse cardiac remodelling. Cell. Signal. *76*, 109770.
39. Knopp, R.C., Jastaniah, A., Dubrovskyi, O., Gaisina, I., Tai, L., and Thatcher, G.R.J. (2021). Extending the Calpain-Cathepsin Hypothesis to the Neurovasculature: Protection of Brain Endothelial Cells and Mice from Neurotrauma. ACS Pharmacol. Transl. Sci. *4*, 372–385.
40. Siklos, M., BenAissa, M., and Thatcher, G.R.J. (2015). Cysteine proteases as therapeutic targets: does selectivity matter? A systematic review of calpain and cathepsin inhibitors. Acta Pharm. Sin. B *5*, 506–519.
41. Heller, L.J., and Katz, S.A. (2000). Influence of enalapril on established pressure-overload cardiac hypertrophy in low and normal renin states in female rats. Life Sci. *66*, 1423–1433.
42. Lahiri, S.K., Lu, J., Aguilar-Sanchez, Y., Li, H., Moreira, L.M., Hulsurkar, M.M., Mendoza, A., Turkieltaub Paredes, M.R., Navarro-Garcia, J.A., Munivez, E., et al. (2024). Targeting calpain-2-mediated junctophilin-2 cleavage delays heart failure progression following myocardial infarction. J. Mol. Cell. Cardiol. *194*, 85–95.
43. Inserte, J., Garcia-Dorado, D., Hernando, V., Barba, I., and Soler-Soler, J. (2006). Ischemic preconditioning prevents calpain-mediated impairment of Na+/K+-ATPase activity during early reperfusion. Cardiovasc. Res. *70*, 364–373.
44. Desmarais, S., Black, W.C., Oballa, R., Lamontagne, S., Riendeau, D., Tawa, P., Duong, L.T., Pickarski, M., and Percival, M.D. (2008). Effect of cathepsin k inhibitor basicity on in vivo off-target activities. Mol. Pharmacol. *73*, 147–156.
45. Liu, Y.-H., Xu, J., Yang, X.-P., Yang, F., Shesely, E., and Carretero, O.A. (2002). Effect of ACE inhibitors and angiotensin II type 1 receptor antagonists on endothelial NO synthase knockout mice with heart failure. Hypertension *39*, 375–381.
46. Garcia-Menendez, L., Karamanlidis, G., Kolwicz, S., and Tian, R. (2013). Substrain specific response to cardiac pressure overload in C57BL/6 mice. Am. J. Physiol. Heart Circ. Physiol. *305*, H397–H402.
47. Poncelas, M., Inserte, J., Vilardosa, Ú., Rodriguez-Sinovas, A., Bañeras, J., Simó, R., and Garcia-Dorado, D. (2015). Obesity induced by high fat diet attenuates postinfarct myocardial remodeling and dysfunction in adult B6D2F1 mice. J. Mol. Cell. Cardiol. *84*, 154–161.

STAR★METHODS

KEY RESOURCES TABLE

REAGENT or RESOURCE	SOURCE	IDENTIFIER
Antibodies		
Alexa Fluor™ 488 goat anti-rabbit	Invitrogen	#A11008 RRID:AB_143165
Calpain-1	Thermo Fisher Scientific	#MA3-940; RRID:AB_2069338
Calpain-2	Abcam	#ab39165; RRID:AB_725844
CD31	Abcam	#ab182981; RRID:AB_2920881
CD45	Abcam	#ab10558; RRID:AB_442810
α-fodrin	Enzo Life Sciences	#BML-FG6090-0100; RRID:AB_2050678
GAPDH	GeneTex	#GTX112699; RRID:AB_11174761
Junctophilin-2	Thermo Fisher Scientific	#40–5300; RRID:AB_2533471
Junctophilin-2	Invitrogen	#PA5-85866 RRID:AB_2802667
Chemicals, peptides, and recombinant proteins		
Angiotensin II	Merck	#A9525
Balicatib	Tocris Bioscience	#5585
Enalapril	Sigma-Aldrich	#E6888
Evans Blue	Sigma-Aldrich	#E2129
NPO-2270	Landsteiner Genmed	N/A
PEG400	Sigma-Aldrich	#91893
Prolong Gold antifade mounting reagent	Thermo Fisher	#P10144
TRIsure™ reagent	Bioline	#BIO-38032
Triphenyltetrazolium chloride (TTC)	Sigma-Aldrich	#T8877
TWEEN80	Sigma-Aldrich	#P4780
Z-VVR-AMC	Enzo Life Sciences	#BML-P199-0010
Critical commercial assays		
cathepsin B activity assay	Eurofins Discovery Services	#178
cathepsin C activity assay	Eurofins Discovery Services	#112300
cathepsin H activity assay	Eurofins Discovery Services	#112550
cathepsin K activity assay	Eurofins Discovery Services	#112600
cathepsin L activity assay	Eurofins Discovery Services	#802
cathepsin S activity assay	Eurofins Discovery Services	#112750
cathepsin V activity assay	Eurofins Discovery Services	#112800
cathepsin Z activity assay	Eurofins Discovery Services	#931
EnVision Detection SystemsPeroxidase/DAB, Rabbit/Mouse	Agilent Technologies	#K5007
SafetyScreen44™ Panel	Eurofins	#P270
Experimental models: cell lines		
HEK293T	ATTC	#CRL-3216
Experimental models: Organisms/strains		
Sprague-Dawley rats (male)	Janvier Labs	N/A
C57BL/6J mice (male)	Janvier Labs	N/A
C57BL/6N mice (male)	Janvier Labs	N/A
Software and algorithms		
Phoenix WinNonlin 6.3	Certara	N/A
SigmaPlot 10.0	Grafiti	N/A
SPSS 20	IBM	N/A

EXPERIMENTAL MODEL AND STUDY PARTICIPANT DETAILS

Cell line

Human embryonic kidney cells (HEK293T) were obtained from ATCC (Manassas, VA, USA). Cultures were maintained in Dulbecco's Modified Eagle Medium (DMEM) (Gibco, USA) supplemented with 10% fetal bovine serum and 1% penicillin-streptomycin (Gibco, USA), at 37°C in humidified atmosphere with 5% CO2. Cell line was tested for mycoplasma contamination prior to use.

Animals

Male C57BL/6JRj and C57BL/6NRj inbred strain mice (25–30 g and 10–12 weeks of age) and Sprague–Dawley (RjHan:SD) outbred strain rats (200–250 g, 6–7 weeks), obtained from Janvier Labs (France), were used in this study. Animals were housed in the animal facility at Vall Hebron Institut de Recerca (VHIR), exposed to 12-h light/dark cycles starting at 8:00 a.m. in temperature (22 ± 2°C) and humidity (55 ± 10%) controlled environment. Animals had *ad libitum* access to food (SAFE 150, Safe Diets, France) and water. The study conforms to the NIH Guide for the Care and Use of Laboratory Animals (NIH publications Nº. 85–23, revised 1996), was performed in accordance with European legislation (Directive 2010/63/UE) and was approved by the Animal Research Ethics Committee of the VHIR (CEEA 45/20 and CEEA 67/19). Animals were randomly assigned to experimental groups.

Ex vivo model of ischemia/reperfusion

Sprague–Dawley rats were euthanized by a lethal i.p. injection of sodium pentobarbital (100 mg/kg). Hearts were excised, retrogradely perfused with modified Krebs-Henseleit buffer in a constant-flow Langendorff apparatus and left ventricular pressure continuously recorded, as previously described.[43] After 20 min of normoxic perfusion, hearts were subjected to 40 min of global ischemia followed by 60 min of reperfusion. NPO or 0.05% DMSO (control group) was added to the perfusion buffer at different concentrations (0.01, 0.1, 1 and 10 μmol/L, n = 6–9 mice per group) during the first 15 min of reperfusion. Cell death was evaluated by measuring lactate dehydrogenase (LDH) activity in the coronary effluent, and infarct size by incubating heart slices in triphenyltetrazolium chloride (TTC; Sigma-Aldrich) as previously described.[43]

In vivo models of acute reperfusion injury and post-infarction remodeling

C57BL/6J mice were anesthetized with pentobarbital (40 mg/kg i.p.) and ketamine (50 mg/kg i.p.), and mechanically ventilated (SAR-830/AP, CWE). A left mini-thoracotomy was performed and mice were subjected to 45 min of ischemia by left anterior descending coronary artery (LAD) ligation and euthanized by a lethal i.p. dose of sodium pentobarbital (100 mg/kg) after 24 h of reperfusion. Infarct size was calculated as the percentage of necrosis (measured by TTC) at the region at risk (measured by Evans blue dye). Mice received a single i.p. injection of NPO (5 or 20 mg/kg, $n = 6$ per group) or its vehicle (5% Tween80, 15% PEG400 in saline, $n = 6$) 10 min before starting reperfusion. To determine the relative contribution of cathepsins to reperfusion injury, an additional group of mice was treated with the cathepsin inhibitor balicatib (Tocris Bioscience) at 25 mg/kg ($n = 5$). At this dose balicatib inhibits cathepsins K, B, L and S.[44] The inhibition of cathepsins by balicatib was confirmed by measuring the fluorescence resulting from the cleavage of the cathepsin substrate Z-VVR-AMC (Enzo Life Sciences) in heart homogenates obtained from mice receiving balicatib.

To analyze the effect of NPO on post-infarction remodeling and heart function, the reperfusion period was extended to 28 days in additional experiments.[8] Based on the results obtained in the acute model, mice were randomly divided to receive over 4 weeks a daily oral gavage dose of 20 mg/kg NPO, its vehicle or 20 mg/kg enalapril (n = 7–8 per group). This dose of enalapril has been reported to reduce post-infarction remodeling in mice.[45]

Angiotensin II treatment

C57BL/6J mice were anesthetized with isoflurane and an osmotic mini-pump (Alzet, model 2002) was implanted subcutaneously to infuse angiotensin II (Sigma-Aldrich) at a dose of 1 μg/kg/min for 14 days. Mice received a daily oral dose of NPO (1, 3, 10 or 30 mg/kg; n = 5–6 per group) or its vehicle (5% Tween80, 15% PEG400 in saline; $n = 6$) for the same time period. After 2 weeks, mice were euthanized by a lethal i.p. dose of sodium pentobarbital (100 mg/kg).

Transverse aortic constriction

C57BL/6J mice were anesthetized with ketamine/xylazine (100 mg/kg-10 mg/kg) and mechanically ventilated. The transverse aortic arch was ligated by tying a 6-0 silk suture around the aorta and a 27G needle to yield a partial and reproducible constriction when the needle was removed. In sham animals, the aortic arch was visualized but not banded. Thorax was closed and analgesia was administrated by buprenorphine (0.1 mg/kg) every 12 h until 48 h.

Mice were randomly divided to receive a daily oral gavage dose of 10 mg/kg NPO (NPO-3w, $n = 10$), 10 mg/kg enalapril (Ena-3w, $n = 10$) or the combination of both treatments (N + E, $n = 6$) from 1 to 4 weeks after TAC surgery. In an additional group, NPO administration started at the time of TAC surgery (NPO-4w, $n = 10$). Sham ($n = 9$) and control group (C-4w, $n = 10$) received NPO vehicle (SF, 5%Tween80, 15% PEG400) during 4 weeks. The NPO-concentration selected was based on the results obtained in angiotensin II-treated mice. To compare the potency of NPO relative to enalapril, we used the same dose for both drugs. At the dose used, enalapril has been shown to attenuate cardiac remodeling induced by TAC.[21]

Mice were euthanized 4 weeks after surgery by a lethal i.p. dose of sodium pentobarbital (100 mg/kg), except a control group that was euthanized after 1 week (C-1w, $n = 6$).

In a series of additional experiments, it was determined whether the administration of NPO prevents the progression of already established HF. For this purpose, the C57BL/6N mouse strain was used since it has been reported that this strain develops HF earlier than the 6J strain.[46] NPO treatment (10 mg/kg) started 2 weeks after TAC surgery and continued for the following 3 weeks ($n = 6$) and echocardiographic data and HW/TL was compared to control group ($n = 7$). Mice were euthanized 5 weeks after TAC surgery by a lethal i.p. dose of sodium pentobarbital (100 mg/kg).

METHOD DETAILS

Cysteine protease inhibition assays

Calpain and cathepsin inhibitory activities of NPO were determined by using kinetic fluorescence assays. Calpain-1 and calpain-2 activities were measured in lysates from HEK293T cells transfected with human *CAPN1+CAPNS1* or *CAPN2+CAPNS1* expressing plasmids as previously described.[9] Cathepsin activity assays were conducted by Eurofins Discovery Services (cathepsin B: #178; cathepsin C: #112300; cathepsin H: #112550; cathepsin K: #112600; cathepsin L: #802; cathepsin S: #112750; cathepsin V: #112800; cathepsin Z: #931).

Pharmacokinetic properties of NPO-2270

The *in vivo* pharmacokinetic characterization of NPO was performed in C57BL/6J mice ($n = 3$ per time point) following a single intravenous (1 mg/kg) or oral (10 mg/kg) administration. Blood samples were collected at 0.08, 0.25, 0.5, 1, 2, 4, 8, 12 and 24 h post intravenous dose and 0.25, 0.5, 1, 2, 4, 6, 8, 12 and 24 h post oral dose. Plasma concentration of NPO was determined by the fit-for-purpose LC-MS/MS method and non-compartmental analysis module in Phoenix WinNonlin (Version 6.3) was used to assess the pharmacokinetic parameters.

Preliminary safety and toxicology studies

NPO was studied at 10 μmol/L concentration in a general safety *in vitro* screen panel including 44 targets (Eurofins Safety Screen44 Panel; #P270).

A short-term repeated-dose toxicity study was performed in male C57BL/6J mice. Mice received daily intraperitoneal (i.p.) administration of NPO at the doses of 10, 30, and 100 mg/kg/day, or its vehicle (5% Tween80, 15% PEG400 in saline) ($n = 3$ per group) for 4 consecutive days. Parameters evaluated during the study included in-life observations such as clinical sign observations, body weights, food consumption, functional observational battery, and gross pathology.

Echocardiography

All echocardiographic studies were performed using a Vivid Q portable ultrasound system with an i12L-RS 13 MHz transducer (GE Healthcare) as described earlier.[47] The left ventricular end-systolic (LVESd) and end-diastolic (LVEDd) internal diameters, interventricular septum thickness (IVST) and left ventricular posterior wall thickness (LVPWT) were measured in M-mode recordings. Left ventricular ejection fraction (EF) was calculated according to standard formulas. For each parameter, measurements were performed from three to six different cardiac cycles, and the values were averaged.

Histology, immunohistochemistry, western blot and RT-PCR

Hearts were fixed in buffered 4% paraformaldehyde and embedded in paraffin for histological evaluation. Collagen deposition was determined in sections at the papillary muscles level stained with Picrosirius red (Sigma-Aldrich) as previously described.[47] Six random photomicrographs from each heart ($n = 6$) were taken at ×200 magnification.

Heart sections corresponding to TAC groups were probed with anti-CD45 (Abcam, #ab10558) and anti-CD31(Abcam, #ab182981) for evaluation of infiltration of inflammatory cells and cardiac vascularization respectively. Slides were incubated with a secondary antibody and visualized with 3,3′-diaminobenzidine (DAB) using the Dako REAL EnVision Detection System (Agilent, #K5007). Photomicrographs were taken at ×400 magnification.

The mean cardiomyocyte cross-sectional area was measured in transverse sections stained with hematoxylin and eosin to evaluate cardiomyocyte hypertrophy. At least 50 random cells from each heart ($n = 5$ per group) were measured at ×400 magnification.

In vivo calpain activity, evaluated by measuring the 145/150 kDa α-fodrin calpain-dependent breakdown products, calpain protein quantification and junctophilin-2 cleavage were assessed by Western blot as previously described.[25] Primary antibodies used were raised against calpain-1 (Thermo Fisher Scientific, #MA3-940), calpain-2 (Abcam, #ab39165), α-fodrin (Enzo Life Sciences, #BML-FG6090-0100), GAPDH (GeneTex, #GTX627408) and junctophilin-2 (Thermo Fisher Scientific, #40–5300).

Markers of fibrosis, hypertrophy and inflammation were quantified by using real-time PCR. Total RNA was extracted using TRIsureTM reagent (Bioline, Meridian Bioscience Inc.) following the manufacturer's protocol. Quantitative RT-PCR was performed using TaqMan universal PCR master mix (Applied Biosystems). The amplification program consisted of 50°C for 2 min, 95°C for 10 min and 40 cycles of 95°C for 15 s and 60°C for 1 min and was performed in a 7900HT Fast Real-Time PCR System (Applied Biosystems). Primers used for BNP, Myh7; Col1A1, Col3A1, Ccl2, Il1b, Il6, Tnf and GAPDH were purchased from Thermo Fisher Scientifc (Mm01255770_g1, Mm00600555_m1, Mm00600555_m1, Mm01254476_m1, Rn00580555_m1, Mm00434228_m1, Mm00446190_m1, Mm00443258_m1 and Mm99999915_g1, respectively).

Imaging of junctophilin-2

Hearts were fixed in 4% PFA, cryopreserved with sucrose gradient, embedded in OCT and frozen in isopentane. Cryosections were permeabilized with 0.25% Triton in blocking buffer and immunolabeled with JP2 polyclonal antibody (PA5-85866, Invitrogen) and secondary antibody conjugated to fluorescent dye (Alexa Fluor 488 goat anti-rabbit, Invitrogen A11008). Nuclei were stained with 5 μg/mL Hoescht 33342 in Prolong Gold antifade mounting reagent (P10144, Thermo Fisher Scientific).

Three-dimensional (xyz) images of 12-micron cryosections were acquired using a Zeiss LSM980 confocal microscope with Airyscan, using a 100× objective (APO NA 1.46). Intensity plot profiles along the entire X axis were analyzed using Python, selecting the maximum peaks allowed within the analysis for measurements. As an admission criterion, peaks were included if their height was higher than 20% and their prominence was higher than 16% of the maximum intensity. Peak intensity and coefficient of variation (CV), as a measure of relative variability and defined as the ratio of the standard deviation to the mean, were quantified. The measurements are expressed as the mean of the values obtained throughout the image scan.

QUANTIFICATION AND STATISTICAL ANALYSIS

Data analysis was performed using SPSS for Windows. Means between groups were compared by one-way ANOVA. Tukey's test was applied as post hoc test when significant differences were observed. Repeated measures ANOVA and Tukey post hoc test were used to compare temporal differences in echocardiographic parameters. The assumption of normality was examined before the statistical analysis using the Shapiro–Wilk test. $p < 0.05$ was considered to be statistically significant. All results are expressed as mean ± SEM.